Journal of Applied Mechanics Vol. 6, pp. 1179-1188 (August 2003) JSCE

Fiber Bridging Degradation Based Fatigue Analysis of ECC under Flexure

架橋応力劣化に基づいたECCの曲げ疲労解析

Peerapong Suthiwarapirak and Takashi Matsumoto
スティワラピラク ピーラポン*・松本高志**

*Graduate student, M. of Eng., Dept. Civil Eng., The Univ. of Tokyo (Hongo 7-3-1, Bunkyo-ku, Tokyo 113-8656)
** Ph.D., Associate Professor, Dept. Civil Eng., The Univ. of Tokyo (Hongo 7-3-1, Bunkyo-ku, Tokyo 113-8656)

This paper proposes a fatigue analysis method of Engineered Cementitious Composite (ECC) under fatigue flexure by applying the concept of fiber bridging degradation. The mechanical degradation of materials under fatigue load is considered a major factor for fatigue crack propagation and subsequent fracture. FEM with the concept of both smeared crack and discrete crack is introduced for representing the consequences of multiple cracks and a localized crack, respectively. The bridging stress degradation law under fatigue load as well as the constitutive relation under static load is introduced as essential input material properties in the fatigue analysis. In order to verify the fatigue analysis, a flexural fatigue test program of two kinds of ECC, PVA-ECC and PE-ECC, was conducted. The fatigue characteristics of flexural beams predicted by the proposed model such as S-N relation and the evolution of midspan deflection agree well with those from the test results. It is also shown that the fatigue analysis is applicable to determine the bridging stress degradation relation of ECC by flexural fatigue tests.

Key Words: ECC, bridging stress degradation, fatigue analysis, fatigue life, S-N relation

1. Introduction

Engineered Cementitious Composite (ECC), an example of cementitious composites mixed with discontinuous fibers, is developed following the concepts of fracture mechanics and micromechanics so that pseudo strain-hardening behavior can be obtained. ECC exhibits very high strength and outstanding tensile strain capacity. For example, ECC that contains less than 2% volume fraction of polyethylene fibers can achieve 5% tensile strain capacity at failure[1]. According to these remarkably improved mechanical properties, ECC is expected to be introduced for several infrastructure applications in the near future.

The high tensile strain capacity and multiple cracking characteristics of ECC even under fatigue loading provide the possibility of applying ECC in the repair of fatigue intensive structures, such as RC bridge slabs. This leads to the necessity of the development of an analytical tool that is applicable to the prediction of structural fatigue performances and to the design of structural repairs in the future.

In the development of the fatigue analysis method, the failure of ordinary cementitious materials, such as plain concrete or Fiber Reinforced Concrete (FRC), under fatigue flexure or fatigue tension is governed by the initiation and the propagation of a single localized crack; therefore, the fictitious crack approach is appropriate and enough for representing the crack and the failure mechanism. The fatigue analysis based on the fictitious crack concept has been successfully developed for predicting the fatigue life and fatigue characteristics of RC beams as well as reinforced FRC beams[2]. However, in the case of ECC under fatigue tension, its failure mechanism is governed not only by a single localized crack, but also by multiple cracks and their propagation[3), 4)]. Multiple cracks are distributed in the tensile zone of the beam before a localized crack takes place. The distribution of these multiple cracks slow down the initiation of a localized crack, and it leads to the extension of fatigue life. Therefore, fictitious crack concept only is not adequate for reproducing the failure mechanisms and fatigue life. In this study, the concept of

smeared crack approach is introduced for representing the effects of multiple cracking processes.

The objective of this study is to propose an analytical model considering the effects of multiple cracks as well as a localized crack in order to predict the fatigue performances of ECC under fatigue flexure. Two types of ECC with two different fibers: polyvinyl alcohol (PVA) and polyethylene (PE) were tested under fatigue flexure, and they are used for the verification of the analytical model. The S-N relation and the evolution of midspan deflection predicted by the analytical model are compared to those from experiments.

2. Fatigue Analysis of ECC Flexural Beams

The development of fatigue analysis of ECC flexural beams and the governing material relations are discussed in this section. In order to reproduce the failure process and predict the structural properties of ECC by an analytical approach, the failure mechanism observed from flexural fatigue experiments is considered in the modeling. The consequent initiations and propagations of both multiple fine cracks and a large localized crack are taken into account as major mechanisms in the analytical model.

For material relations, the material degradation law under fatigue loading is considered the essential cause of crack propagation. For mechanical degradation, after a crack initiates in ECC, the transferred stress across crack occurs due to fiber bridging action. When fatigue loading is applied, the transferred stress across cracks reduces according to the degradation of the fiber bridging. This mechanism is so called "Bridging Stress Degradation".

2.1 Modeling

An FEM model is proposed incorporating the above described fatigue failure mechanism. It is found from the flexural fatigue experiment[5), 6)] that the flexural fatigue failure of the ECC involves three stages: the initiation of multiple cracks, the propagation of those cracks, and the propagation of a localized crack. At a small number of fatigue loading cycles, multiple cracks initiate along the flexural span as well as into shear span of the specimen, then those cracks propagate stably and lead to a gradual increase in midspan deflection of the specimen. Finally, only one crack localizes, and it induces the final failure of the specimen.

The analytical model is proposed by combining both smeared crack and discrete crack concept. Smeared crack elements are introduced for representing the multiple cracking process, and discrete crack elements or interface elements are used for representing the localized cracking process.

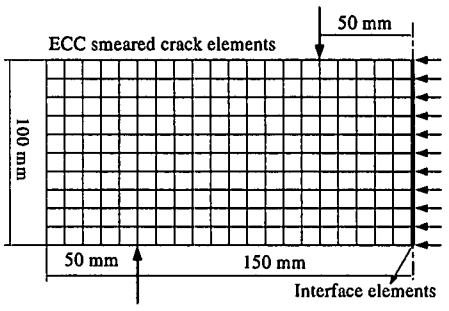

Fig. 1 FEM mesh for ECC flexural fatigue analysis

Fig. 1 shows the finite element mesh of ECC beams under four-point bending load. The model consists of smeared crack elements for distributed cracks and interface elements for a localized crack at the center of the ECC specimen. The degradation of bridging stress of smeared crack elements under fatigue loading leads to the initiation of new cracks. With the increase in the number of loading cycles, the initiation of new cracks and the propagation of existing cracks proceed and they are represented by the expansion of a fracture zone of smeared crack elements. The degradation of bridging stress across the crack in interface elements causes the propagation of the localized crack and it leads to the final failure of the beam.

2.2 Material model development

The constitutive relation of a material under static loading is considered an input in FEM analysis under static loading. In a similar manner, for fatigue analysis, material property that represents the degradation of bridging stress of cracks under fatigue loading is essential. In this study, the bridging stress degradation law of ECC under fatigue load is discussed based on micromechanics of fibers. Then, the simplified degradation relation is proposed for the fatigue analysis.

(1) Constitutive relation of ECCs

The constitutive relation of ECCs under static loading was obtained from the uniaxial tension test. It is defined as the relation between tensile stress, σ_t, and tensile strain, ε_t, or crack width, δ.

For smeared crack elements, the constitutive relation that is the relation between the tensile stress, σ_t, and tensile strain, ε_t, is introduced. For discrete crack elements or so called interface elements, the relation of tensile stress, σ_t, and crack width, δ, is adopted.

The constitutive relation of both PVA-ECC and PE-ECC are obtained from the average value of uniaxial tensile test specimens under static loading, and they are shown in **Fig. 2**.

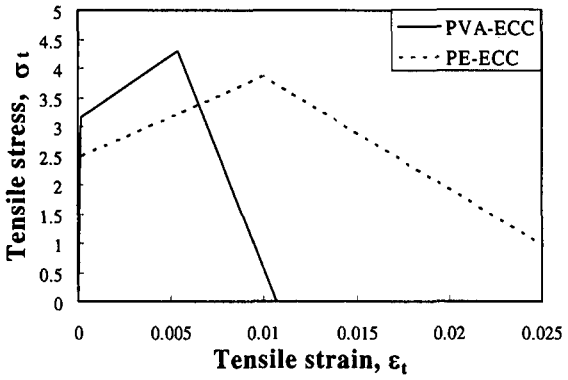

Fig. 2 Constitutive relations of ECCs under static loading

(2) Micromechanics based bridging stress degradation law

The bridging stress degradation of cracks under fatigue load promotes the crack propagation mechanism and its consequent failure in ECC. After a crack initiates on the tension side of a specimen at the first loading, it can sustain tensile loading without sudden failure because of their Pseudo Strain Hardening and the transfer of bridging stress across each crack occurring due to fiber bridging action. The initiation of new multiple cracks and the propagation of a localized crack under fatigue loading induce the failure of ECC.

From the viewpoint of micromechanics, the failure of ECC under fatigue flexure is governed by the fiber bridging characteristics[5]. The investigation of fibers on the crack plane of fractured specimens shows that fibers exhibited rupture failure as well as pullout. The stress degradation is caused by two main fiber-bridging characteristics: the fiber/matrix interfacial bond degradation and fiber fatigue rupture.

Interfacial bond degradation: In fiber reinforced cementitious composites, fibers exhibit bridging stress degradation, which is mainly due to the fiber/matrix interfacial damage or the decay of bond strength between fiber and matrix[7]. The bond strength degradation is assumed to be a function of the number of loading cycles, N, initial bond strength, τ_1, and the amplitude of fiber reverse slippage, $\Delta\delta$ (which corresponds to the amplitude of crack width).

$$\frac{\Delta\tau_{N+1}}{\tau_1} = f(N, \Delta\delta_N) = k\Delta\delta_N \qquad (1)$$

where τ_{N+1} is the bond strength reduction after N+1 cycles. k is the normalized bond reduction coefficient which is cycle dependent. It is assumed that k obeys a bi-linear function of log(N)[7], and the first slope of k is higher than the second. This means interfacial bond degrades faster in the low number of cycles.

Fiber fatigue rupture: Under cyclic fatigue loading, the rupture of fibers takes place even when the tensile stress of fiber has not reached the tensile strength of fiber. In fiber cementitious composites, the exposed fibers along a crack plane under cyclic fatigue loading that show higher tensile stress level fail earlier by fatigue rupture. The rupture failure leads to the decrease of stress transfer across crack. Fiber fatigue rupture is considered to be dependent on the number of cycles, N, and tensile stress level, σ_t.

The bridging stress degradation law that considers fiber fatigue rupture can be expressed as a function of several parameters as given by[8]:

$$\frac{\sigma_N}{\sigma_1} = f(\alpha, \alpha_f, \beta_f, \tilde{\delta}^*, N^*)$$
$$\tilde{\delta}^* = \frac{\delta^*}{(L_f/2)}; \qquad \delta^* = \frac{\tau L_f^2}{E_f d_f} \qquad (2)$$
$$\alpha = \frac{\delta}{\delta^*}; \quad \alpha_f = \frac{\delta_{max}}{\delta^*}; \quad \beta_f = \frac{\Delta\delta}{\delta_{max}}$$

where σ_N and σ_1 is defined as the bridging stress after N cycles of fatigue loading and the bridging stress at the first cycle, respectively. The term δ is defined as crack width, and δ_{max} is the maximum crack width under fatigue loading. E_f and d_f are the Young's modulus and diameter of fibers. τ is the interfacial bond strength between fiber and matrix. $\Delta\delta$ is defined as the amplitude of crack width under fatigue loading. N* is the normalized number of loading cycles. It is defined as

$$N^* = \frac{NL_f}{L_c}$$
$$L_c = \frac{\sigma_{fu} d_f}{4\tau} \qquad (3)$$

here, L_f is fiber length and σ_{fu} is the tensile strength of fiber. It is noted that besides the fiber properties, the bridging stress is governed by two main parameters; crack width, δ and the number of cycles, N.

The development of the micromechanics based bridging stress degradation model considering both fiber fatigue rupture and interfacial bond degradation can provide the bridging stress degradation relation for general cases of ECC. However, at present, such a model has not been completely developed yet. Therefore, it is necessary to adopt a simplified model in order to introduce as an input of the analysis in this study. As discussed earlier, the stress degradation law of materials depends mainly on two kinds of parameters

corresponding to tensile strain, ε_t (or crack width, δ) and to the number of cycles, N. In this study, the stress degradation law is assumed based on these two parameters and it will be discussed in the next section.

(3) Simplified bridging stress degradation law for fatigue life analysis

ECC under uniaxial fatigue tensile test with constant tensile strain exhibited the degradation of tensile stress with the increase in number of loading cycles[9]. At first static loading, multiple cracks occurred. During subsequent fatigue loading, fiber bridging degraded due to fiber fatigue rupture. This leads to the degradation of bridging stress of those cracks. For higher applied tensile strain, initial crack width was larger and the initial fiber stress was higher. Therefore, fibers were broken easier due to fiber fatigue rupture. The bridging stress degradation law of ECC is then simplified to relate to only two essential parameters, number of loading cycles, N, and tensile strain, ε_t (or crack width, δ). In order to represent two kinds of cracks, distributed cracks and a localized crack, the bridging stress degradation law is categorized into 2 kinds of elements: the relations for smeared crack elements and interface elements, respectively.

Degradation law for smeared crack elements: The bridging stress degradation is considered to occur by multiple cracks in smeared crack elements. The ECC degradation law for these elements can be simply assumed by the relation between tensile stress and tensile strain, and it is shown by:

$$\frac{\sigma_N}{\sigma_1} = f(\varepsilon_t, N)$$
$$\frac{\sigma_N}{\sigma_1} = 1-(k_1 + k_2\varepsilon_t)Log_{10}N \quad (4)$$

The degradation law of multiple cracks in ECC represented by smeared crack elements can be illustrated as shown by **Fig. 3**. The degradation law is assumed to be related to two coefficients for each material, k_1 and k_2 as shown in Eq. (4). The coefficients k_1 and k_2 of the level of dependencies on the number of cycles, N, and tensile strain, ε_t, respectively.

When k_1 is large, the degradation of material is N-dominant relation and when k_2 is large, the degradation of materials is much affected by the tensile strain level, ε_t. The bridging stress degradation rate is large when k_1 and k_2 are large.

Degradation law for interface elements: After crack localization, the bridging stress degradation is caused by the bridging stress degradation of the localized crack.

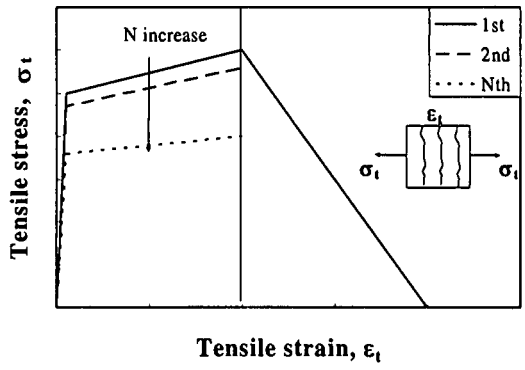

Fig. 3 Degradation law of smear crack elements

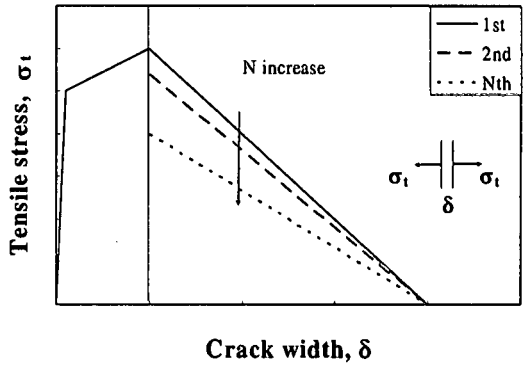

Fig. 4 Degradation law of interface elements

The stress degradation law for interface elements is defined as the relation between tensile stress and crack width, δ.

$$\frac{\sigma_N}{\sigma_1} = f(\delta, N)$$
$$\frac{\sigma_N}{\sigma_1} = 1-(k_1 + k_2\delta/l_e)Log_{10}N \quad (5)$$

The degradation law of a localized crack in ECC represented by interface elements can be illustrated as shown by **Fig. 4.**

It is noted that the tensile strain, ε_t (Eq. (4)) and the crack width, δ (Eq. (5)) can be related to each other by considering the length of elements, l_e ($\varepsilon_t = \delta/l_e$). In other words, Eq. (4) and (5) become the same equation.

2.3 Procedure of fatigue analysis

The procedure of fatigue life analysis is shown by a simply supported ECC beam subjected to a fatigue load **(Fig. 5(a))**.

The constant fatigue load, P_N, which is below the ultimate load, is applied in the fatigue life analysis. At

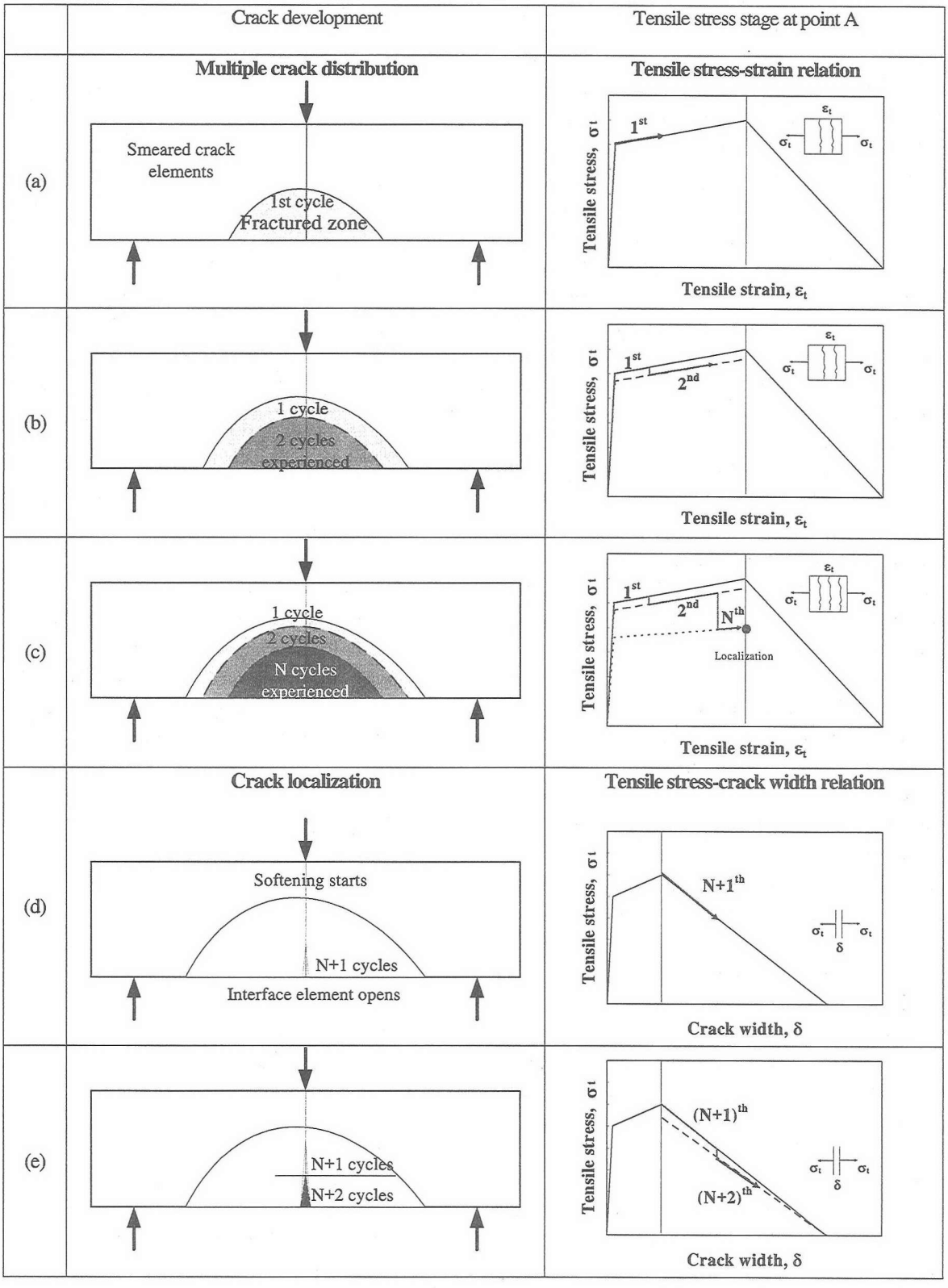

Fig. 5 Fatigue analysis process and crack development under fatigue loading

low number of cycles, the stress degradation of distributed cracks is dominant. At the first cycle, distributed cracks initiate, and they are represented by the fractured zone of smeared crack elements shown in **Fig. 5(a)**. When P_N at the second cycle is applied, the cracks in the fractured zone that initiated at the first cycle experiences tensile stress for the second time. This leads to the degradation of transferred stress in the fractured zone (**Fig. 5(b)**). The change of stress stage can be illustrated as shown by the degradation of stress and the increase of tensile strain at point A. In order to obtain new equilibrium, fractured zone have to propagate more

for new tensile stress transfer area.

With the increase of number of loading cycles, the tensile strain at the point A increase and the fractured zone enlarges its size (**Fig. 5(c)**). When the number of cycles increases, tensile strain becomes larger and it reaches the softening strain. At this moment, interface elements which represent a localized crack play an important role. The extension of the fractured zone by smeared crack elements ceases, while interface elements open rapidly (**Fig. 5(d)**). The degradation bridging stress of interface elements leads to the significant increase of crack width of a localized crack. The localized crack propagates both by increase length and width with the increase of applied loading cycles (**Fig. 5(e)**) until the equilibrium for this beam cannot be satisfied with further crack propagation. At this moment, the beam fails, and it defines the fatigue life. The cycles to failure (N_u) can therefore be obtained for each fatigue stress level.

It is noticed that only the stress degradation at the maximum loading of each fatigue loading cycle is taken into accounts in this study; therefore, the unloading and reloading paths of constitutive relation is not considered in the analysis model.

2.4 Input for fatigue analysis

The material models shown in section 2.2 are considered as inputs for the fatigue analysis. The constitutive relation under static loading illustrated in **Fig. 2**, and the bridging stress degradation relations shown by Eq. (4) and Eq. (5) are adopted for the analysis. The Young's modulus and Poisson's ration of ECC in the analysis are $2x10^4$ MPa and 0.17 respectively.

3. Flexural Fatigue Test

3.1 Materials and specimens

Static and fatigue flexure experiments were conducted for two types of ECCs: one reinforced with polyvinyl alcohol (PVA) fibers and the other with polyethylene (PE) fibers. These two ECCs are hereinafter referred to as PVA-ECC and PE-ECC, respectively. The properties of these two fiber types are shown in **Table 1**. The mix proportion was the same for both ECCs, and it is shown in **Table 2**.

A wet mixed shotcrete method was employed to fabricate the beam specimens with depth 100mm, thickness 100mm, and length 400mm. 22 specimens for PVA-ECC and 15 specimens for PE-ECC were shotcreted into formworks. After the fabrication, all specimens were moist cured under the constant temperature of 20 degrees Celsius and relative humidity of 60%. The age of specimens at testing is at least two months so as to alleviate the effect of initial hydration development.

Table 1 Properties of fibers[10)]

ECC type	PVA-ECC	PE-ECC
Fiber type	PVA fibers	PE fibers
Length (mm)	12	8
Diameter (μm)	40	14
Tensile strength (MPa)	1600	2790
Frictional bond strength (MPa)	2.01	0.66

Table 2 Mix proportion of both ECCs[11)]

Material	W/B*	S/B**	Water (Kg/m^3)	Fiber volume fraction (%)
PVA-ECC	0.32	0.42	382	2.1
PE-ECC	0.32	0.42	382	1.5

* Water-cementitious material ratio

** Sand-cementitious material ratio

3.2 Apparatus and test procedure

The apparatus employed in this study was a 200 kN capacity feed back controlled loading machine. For static loading, the tests were carried out under displacement control condition, while fatigue tests were under load control condition. Four-point flexural tests were conducted both under static loading and fatigue loading. Specimens were simply supported on a clear span of 300 mm and were subjected to two-point load at one-third of the span.

Static flexural test were conducted before fatigue flexural tests under displacement control condition. They were performed in accordance with JCI standard for test methods of FRC (JCI-SF4[12)]). The static flexural strengths of two ECCs were determined. Based on the average flexural strength, the maximum fatigue stress were determined for each level. In order to construct the fatigue stress-life relation (S-N relation), five levels for PVA-ECC and four levels for PE-ECC were conducted.

For flexural fatigue tests, specimens were subjected to an 8 Hz sinusoidal cyclic load. The ratio between the maximum flexural stress and the minimum flexural stress was set constantly equal to 0.2 for all specimens in order to avoid any impact and slip of specimens during testing.

3.3 Data collection

Linear Variable Differential Transducers (LVDTs) were introduced to measure the deflection at the midspan of specimens from both sides of specimens. They were mounted on a steel frame fixed on a specimen so that the displacement evolution produced only by the specimens can be measured.

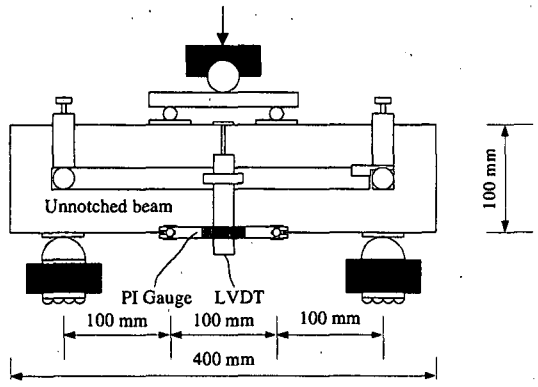

Fig. 6 Experimental set-up

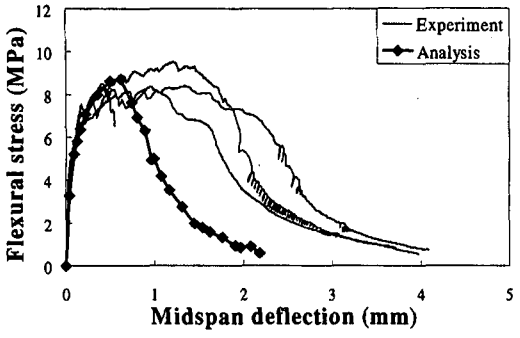

(a)

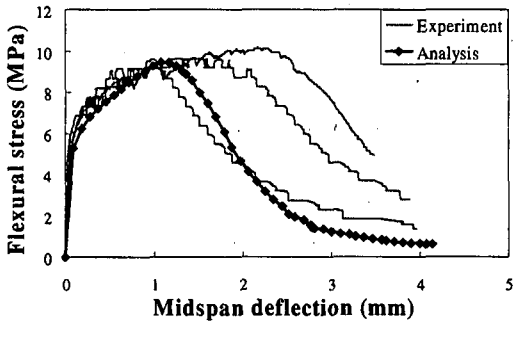

(b)

Fig. 7 Comparison of flexural stress and deflection relation from analysis and experiment a) PVA-ECC b) PE-ECC

Under fatigue loading, measurement data at the maximum stress and the minimum stress levels were recorded. The numbers of cycles at which cracks initiated and the number of cycles at which a specimen failed were recorded for each specimen.

The experimental set-up and measurement devices are shown in **Fig. 6**

4. Analytical and Experimental Results

The experimental and analytical results both under static and fatigue loading are illustrated and discussed in this section. In order to verify the analytical model, the analytical results are compared with the experimental results. It is noted that the experiment results of ECC flexural beams and the discussions of fatigue flexural characteristics are shown in details in reference 5).

Table 3 Ultimate flexural strength from analysis and experiment

Material	Analysis	Experiment
PVA-ECC	8.73	8.71
PE-ECC	9.57	9.93

4.1 Results under static loading

The relation between flexural stress and midspan deflection of four static specimens of PVA-ECC and three static specimens of PE-ECC are shown in comparison with the analytical results in **Fig. 7(a)** and **Fig. 7(b)**, respectively. The ultimate flexural strength of both ECCs from the analysis compared with that from the experiment are shown in **Table 3**. It is found that the analytical results well agree with the experimental results for both the ultimate strength and the stress-midspan deflection relation. The hardening behavior from multiple cracking before the flexural stress drops can be reproduced well by the analysis.

4.2 Results under fatigue loading

Fatigue test results are used for verifying the proposed analysis and for determining the bridging stress degradation relation. In the analytical model, two essential material relations, the constitutive relation under static loading and the bridging stress degradation law, are introduced as input material properties. Then the flexural fatigue characteristics, such as the S-N relation and the evolution of midspan deflection and crack width, can be predicted by the model.

(1) S-N relation

The fatigue stress level and fatigue life relations (S-N relations) of both ECCs were constructed from both experiment and analysis approach. Fatigue stress level, S is defined as the ratio of the maximum stress to the static flexural strength.

The experiment showed that both ECCs exhibited an extended fatigue life at high fatigue stess level (**Fig. 8(a)** and **Fig. 8(b)**). The shape of S-N relation of both ECCs performed a unique characteristic becasuse it showed a mild slope at high fatigue stress level. This means ECC performed an extended fatigue life under high stress level in comparative to other cementitious materials[5].

The bridging stress degradation law of both ECCs are assumed as the relation in Eq. (4) and (5). The bridging stress degradation relation is obtained when the analysis provided the analytical S-N relation to agree with the

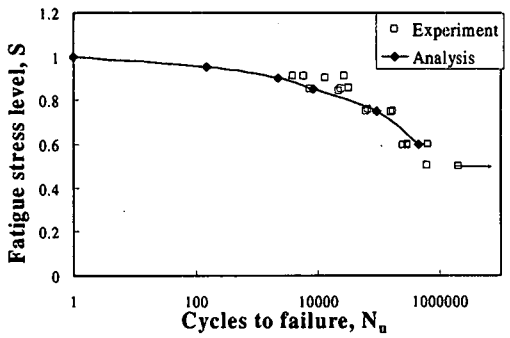

(a)

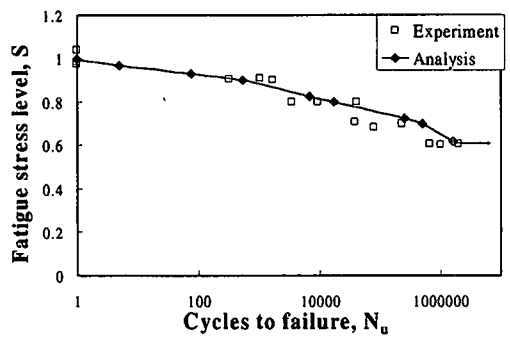

(b)

Fig. 8 S-N relation of a) PVA-ECC and b) PE-ECC

experimental S-N relation. The coefficients k_1 and k_2 (Eq. (4) and (5)) are changed gradually for each trial. When either k_1 or k_2 is increased the fatigue life become shorter, and when k_2 is increased, the slope of S-N relation tends to become more negative with the increase of N. After several trials, the final degradation relations for both two kinds of ECC are shown below.

PVA-ECC

$$\frac{\sigma_N}{\sigma_1} = 1 - (0.025 + 15\varepsilon_t) Log_{10}(N) \qquad (6)$$

PE-ECC

$$\frac{\sigma_N}{\sigma_1} = 1 - (0.030 + 6\varepsilon_t) Log_{10}(N) \qquad (7)$$

It is noticed that the coefficient k_1 in the degradation law of PVA-ECC is smaller, but the paremeter k_2 of PVA-ECC is larger than that of PE-ECC. This implies that PVA-ECC exhibits the bridging stress degradation, which is more dependent on the tensile strain level than that of PE-ECC.

(2) Comparison of damage evolution

The comparison of damage evolution are conducted in order to verify the obtained bridging stress degradation. The evolution of midspan deflection and displacement measured by π gauges are used for this verification.

The evolution of midspan deflection of PVA-ECC and PE-ECC from the experiment is illustrated in **Fig. 9(a)** and **Fig. 9(b)**, respectively. Only one typical specimens for each fatigue stress level is shown. It is found from experiments that the evoltion of midspan deflection depended on fatigue stress level. The midspan deflection of both types of ECC at final failure reduced with the decrease of fatigue stress level.

Table 4 the ratio of ruptured fibers and pull out fibers along arbitrary length

Material	Static	Fatigue
PVA-ECC	2.40	3.20
PE-ECC	0.54	0.59

Fig. 10(a) and **Fig. 10(b)** show the evolution of midspan deflection of PVA-ECC and PE-ECC from the analysis. It is shown that the stress level dependent characteristic is well reproduced by the model. At higher fatigue stress level, the midspan deflection of specimen is higher.

Fig. 11 shows the strain distribution of the fatigue specimen at S=0.80. At the first loading cycle, some distributed cracks occurred in the tension side as shown by the fractured zone under dash line (a). With the increase of number of cycles, the fractured zone expanded. Before the final failure, the localized crack represented by interface elements opened significantly as shown in (b). This conforms to the experiment observation that multiple cracks distributed in the middle span of the beam.

It is found that the proposed analytical method can reproduce the failure mechanism and failure characteristics of ECC beam under fatigue flexure.

5. Discussions

5.1 Bridging stress degradation and fiber bridging characteristics

The fiber characteristics of both ECCs after fatigue failure were investigated with a microscope. It is found that there are two kinds of fiber characteristics on the fracture planes: ruptured fibers due to fatigue and pulled-out fibers due to fiber/matrix interface bond degradation. These two kinds of fiber bridging characteristics were counted for an arbitrary length of 10 mm, and the results are summarized in **Table 4**. The values in the table show the ratio between the numbers of ruptured fibers and pull out fibers. It can be concluded that PVA-ECC is fractured fiber dominant, while PE-ECC is pulled out fiber dominant. Moreover, PVA fibers were severely ruptured under fatigue loading, while PE fibers showed nearly the same ratio both under static loading and fatigue loading.

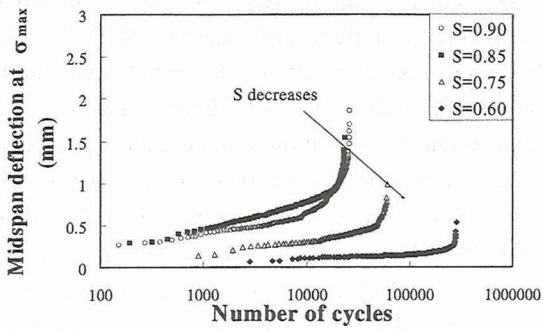

Fig. 9 Evolution of midspan deflection from experiments of a) PVA-ECC and b) PE-ECC

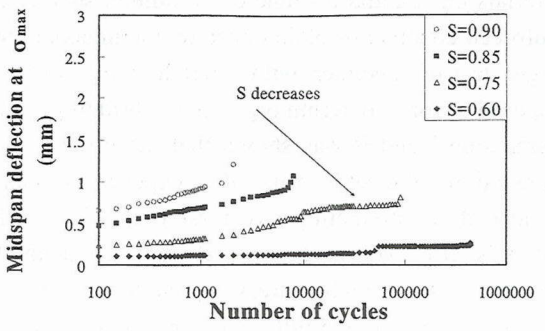

Fig. 10 Evolution of midspan deflection from analysis of a) PVA-ECC and b) PE-ECC

In the viewpoint of fiber bridging characteristics, PVA fibers were subjected to a high fatigue tensile stress level. This leads to the severe rupture of fiber under fatigue and it causes the high rate of decay of bridging stress. The number of fractured fibers depends on the fatigue stress level. This may lead to the conclusion that ECC revealing much fiber rupture exhibits the degradation dominated by tensile strain magnitude.

From the evolution of midspan deflection, it is found that PVA-ECC exhibited more fatigue stress dependent than that of PE-ECC. At a higher fatigue stress level, an initial tensile strain was larger, and it resulted in the higher rate of increase of midspan deflection because of higher rate of expansion of fractured zone. This supports that the degradation of PVA-ECC is more tensile strain dependent than that of PE-ECC. This conforms to the bridging stress degradation relation obtained from the analysis that the stress degradation of PVA-ECC is much dependent on tensile strain level than that of PE-ECC. It can be concluded that the fiber bridging characteristics governs the bridging stress degradation law of ECCs.

5.2 Application of the analytical model for determining bridging stress degradation

The bridging stress degradation relation is one of the essential relations introducing for the prediction of structural behaviors under fatigue. For fiber cementitious

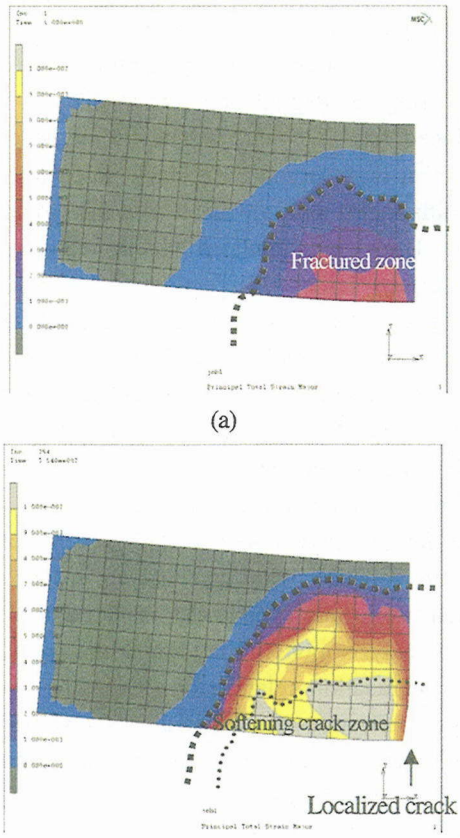

Fig. 11 Principal strain distribution of PE-ECC beam under fatigue (S=0.80) at a) N=1 and b) just before failure

materials that exhibit a single crack failure, such as fiber reinforced concrete or plain concrete, the uniaxial tensile fatigue test of specimen with a notch at the center was proposed for determining the bridging stress degradation[13] and it was shown that the bridging stress degradation obtained from the experiment can be introduced for predicting structural properties of those materials. However, in the case of ECC, the method for determining the bridging stress degradation has not been proposed yet due to the difficulties in fatigue tension test set-up for capturing multiple cracks in a specific area.

This study shows that it is able to introduce the proposed analytical model for determining the bridging stress degradation of ECC. The flexural fatigue test, which is simpler in test setting than uniaxial tension test is conducted in order to investigate flexural fatigue properties of beam. Then, the S-N curve is constructed and the evolution of midspan deflection is recorded. These results are used in curve fitting with the analytical results obtained from the assumed bridging stress degradation relation. The bridging stress degradation is adopted when the analytical results can reproduce the experiment results.

6. Conclusion

A fatigue analysis method of ECC under fatigue flexure has been proposed by applying the concept of fiber bridging degradation. The analysis has been developed based on the fatigue failure mechanism of ECCs that is governed by a crack propagation process. The initiation of multiple cracks and the propagation of a localized crack are simulated by smeared crack elements and interface elements, respectively.

For material relation, the bridging stress degradation law of ECC which considers fiber rupture and fiber/matrix interface bond degradation is discussed and based on this law, the simplified degradation relation which depends on only two parameters N and ε_t, are proposed as the input of the analysis.

The fatigue flexural tests of ECCs were conducted in order to compare with the analysis results. The S-N relation from the experiment is introduced with the fatigue analysis model to determine the fatigue bridging stress degradation relation of ECC. The evolution of midspan deflection was selected for the verification. It is shown that the analytical results can reproduce the evolution characteristics that fatigue stress dependent evolution of midspan deflection.

This study supports that it is able to apply the flexural fatigue test of ECC as an alternative method to determine the bridging stress degradation relation.

For structural application, the analysis model is used for predicting fatigue performances of ECC. When the bridging stress degradation relation is known, the flexural fatigue properties of ECC beams, such as the S-N relation and the evolution of deflection are predictable.

The fiber bridging characteristics, fiber rupture and fiber pull out involves the bridging stress degradation law of ECCs. Therefore, for the further development, the uniaxial tensile fatigue test would be an interesting topic in the sense that it is essential to the development and the verification of micromechanics based bridging stress degradation law.

REFERENCES

1) Li, V. C.: From Micromechanics to Structural Engineering – the Design of Cementitious Composites for Civil Engineering Applications, *Journal of Structural Mechanics and Earthquake Engineering*, No. 471/I-24, pp. 1-12, 1993.
2) Suthiwarapirak, P., Matsumoto, T., and Horii, H.: Fatigue Life Analysis of Reinforced Steel-fiber-concrete Beams, *Proceedings of the Japan Concrete Institute*, Vol. 23, No. 3, pp. 127-132, 2001.
3) Kanda, T. and Li, V. C.: New Micromechanics Design Theory for Pseudostrain Hardening Cementitious Composite, *Journal of Engineering Mechanics*, Vol. 125, No. 4, pp. 373-381, 1999.
4) Kanda T. and Li. V. C.: Effect of Fiber Strength and Fiber-Matrix Interface on Crack Bridging in Cement Composites, *Journal of Engineering Mechanics*, Vol. 125, No. 3, pp. 290-299, 1999.
5) Suthiwarapirak, P., Matsumoto, T., and Kanda, T.: Flexural Fatigue Failure Characteristics of an Engineered Cementitious Composite and Polymer Cement Mortar, *Journal of Cement and Concrete Composites*, Vol. 57, No. 718, pp. 121-134, 2002.
6) Matsumoto, T. Suthiwarapirak, P., and Kanda, T.: Mechanisms of Multiple Cracking and Fracture of DFRCCs under Fatigue Flexure, *Proceedings of the JCI International Workshop on Ductile Fiber Reinforced Cementitious Composites (DFRCC) - Application and Evaluation -*, pp. 259-268, 2002
7) Zhang, J., Stang, H., and Li, V.C.: Crack Bridging Model for Fibre Reinforced Concrete under Fatigue Tension, *International Journal of Fatigue*, Vol. 23, pp. 655-670, 2001.
8) Matsumoto, T, Suthiwarapirak, P., and Asamoto, S.: Model Development of ECC Fatigue Analysis, *Proceedings of the Japan Concrete Institute*, Vol. 24, No. 1, pp. 237-242, 2002 (In Japanese).
9) Chun, P.: Development of a Bridging Stress Degradation Model Accounting for Fiber Rupture and its Validation with ECC Fatigue Tests, Senior Student Thesis, The University of Tokyo, 2003 (In Japanese).
10) Kanda, T. and Li, V. C.: Practical Design Guidelines for Pseudo Strain Hardening Cementitious Composites Reinforced with Short Random Fibers – Part I Micromechanics Theory for Predicting First Cracking Strength, *Journal of Structural and Construction Engineering*, AIJ, 539, pp. 13-21, 2001
11) Kanda, T., Saito, T., Sakata, N., and Hiraishi, M.: Fundamental Properties of Directed Sprayed Retrofit Material Utilizing Fiber Reinforced Pseudo Strain Hardening Cementitious Composites, *Proceedings of the Japan Concrete Institute*, Vol. 23, No. 1, pp. 475-480, 2001.
12) Japan Concrete Institute: *JCI Standards for Test Methods of Fiber Reinforced Concrete*, pp. 45-48, 1984.
13) Zhang, J., "Fatigue Fracture of Fiber Reinforced Concrete- An Experimental and Theoretical Study," Ph.D. Thesis, Department of Structural Engineering and Materials, Technical University of Denmark, 1998.

(Received April 18, 2003)